Received: 25 June 2020 | Revised: 8 December 2020 | Accepted: 9 December 2020

DOI: 10.1002/er.6356

SPECIAL ISSUE RESEARCH ARTICLE

INTERNATIONAL JOURNAL OF ENERGY RESEARCH WILEY

Low-energy nuclear fusion reactions in solids: Experiments

Dimiter Alexandrov

Department of Electrical Engineering, Lakehead University, 955 Oliver Road, Thunder Bay, Ontario, P7B5E1, Canada

Correspondence
Dimiter Alexandrov, Lakehead University, Thunder Bay, Ontario, Canada.
Email: dimiter.alexandrov@lakeheadu.ca

Summary

Replicable experimental results about low-energy nuclear fusion reactions based on initially reacting deuterium nuclei giving cold nuclear fusion synthesis of helium (both isotopes ^{3}He and ^{4}He) and energy release as final products are reported in this article. These final products are results of interaction of deuterium with the solids in experimental system including two specimens: molybdenum metal and palladium nanowires. Experimental proofs about cold nuclear fusion synthesis of both ^{3}He and ^{4}He are provided. It reported a correlation between concentration of the generated helium and the measured temperature of the sample holder. It is found that the concentrations of both ^{3}He and ^{4}He increase with increase of the kinetic energies of the interacting deuterium nuclei and also with increase of the temperature of the sample holder.

KEYWORDS

low-energy nuclear reactions, nuclear fusion, solid-state physics

1 | INTRODUCTION

During the past three decades, the matter about possibility for existence of low-energy nuclear reactions (LENRs) was subject to continuous discussions. One uses the name "low-energy nuclear reaction (LENR)" in consideration that the cold nuclear fusion is part of LENRs although terminology "condensed matter nuclear science" has more modern use at present. The reported results in this article pertain purely to cold nuclear fusion synthesis of two helium isotopes ^{3}He and ^{4}He, and this synthesis is based on interactions of deuterium gas with metals at relatively low temperatures, that is, it is exactly nuclear fusion reaction at relatively low temperatures. In this article, terminology "cold nuclear fusion" as part of LENR is used wherever nuclear synthesis of helium has taken place, and terminology "LENR," otherwise. Since the time when M. Fleischmann and S. Pons reported[1] their results assuming cold nuclear fusion reactions supported by Jones et al,[2] many researchers carried out experiments mainly based on electrolysis of heavy water as the major part of the experiments confirmed the outcomes reported in Reference 1. A minor part of the researchers in this field performed experiments using either vacuum or pressure systems. The experimental results were published at relevant papers mainly in the ICCF conference proceedings (ICCF—International Conference on Cold Fusion) and in very rare cases in other journals (such as[3]). Also, there are few journal articles pertaining to cold nuclear fusion experiments.[4-7]

There is significant number of attempts[8-18] for theoretical explanations of the low-energy nuclear reactions. The purpose of this article is not to do review of the theory in this field, and that is why, one will not express opinion about these theoretical attempts and one will only say that the theoretical outcomes of these papers do not explain completely the observed experimental results that are reported in this article. Even the theory developed in Reference 19 does not apply completely to the obtained experimental results as the observed experimental outcomes, such as increase of the helium concentration with increase of either kinetic energies of the interacting deuterium nuclei or the temperature, cannot be explained by this theory. The above is the reason that one developed new theory explaining cold nuclear fusion in solids as this theory will be published separately.

Experimental results about cold nuclear fusion synthesis of both helium isotopes ^{3}He and ^{4}He on basis of interaction of deuterium nuclei with Mo metal and with Pd nanostructures are reported in this article. Corresponding proofs about this synthesis are provided on basis of both mass analysis and plasma optical spectroscopy. The proofs are of two types—direct and indirect. Dependences of the concentrations of both ^{3}He and ^{4}He on the temperature and on the kinetic energies of the initial interacting nuclei are provided.

2 | DESIGN OF THE EXPERIMENTS AND TREATMENTS OF THE OBSERVED MEASUREMENTS

The experimental reactor consists of two chambers—main chamber and residual gas analyzer (RGA) chamber. Both chambers are connected by flexible pipe equipped with gas pressure regulator maintaining the gas stream from the main chamber into the RGA chamber. (This gas stream is taken by RGA probe in the main chamber.) The main chamber is equipped with separated DC plasma source that can produce plasma by injected deuterium-nitrogen (D_2/N_2) gas mixture (4.5% D_2 and 95.5% N_2) and to inject this plasma in the main chamber through holes. It has a sample holder made by stainless steel. External spectrometer and external radiation detectors (one for neutrons and for gamma rays and another for alpha, beta, and gamma rays) are placed in front of a window of the main chamber. The specific features of the entire system (Figure 1) are:

1. The pressure of the D_2/N_2 gas mixture in the main chamber can be regulated in interval from few mTorr up to 3000 mTorr. During the experiments, the pressure of the deuterium-nitrogen gas mixture in the main chamber was maintained within the interval 100 to 2500 mTorr, and the maximum gas pressure in the RGA chamber was maintained in range $\sim 10^{-7}$ to $\sim 10^{-6}$ Torr. The reason for these relatively low pressures was precise measurements about pressures corresponding to different gases to be done, that is, during all the time the intention was that even small amounts of gases to be detected.
2. The temperature of the sample holder can be measured by both the thermocouple and external pyrometer (it is not shown in the scheme of Figure 1), and there is a heater attached to the sample holder as this

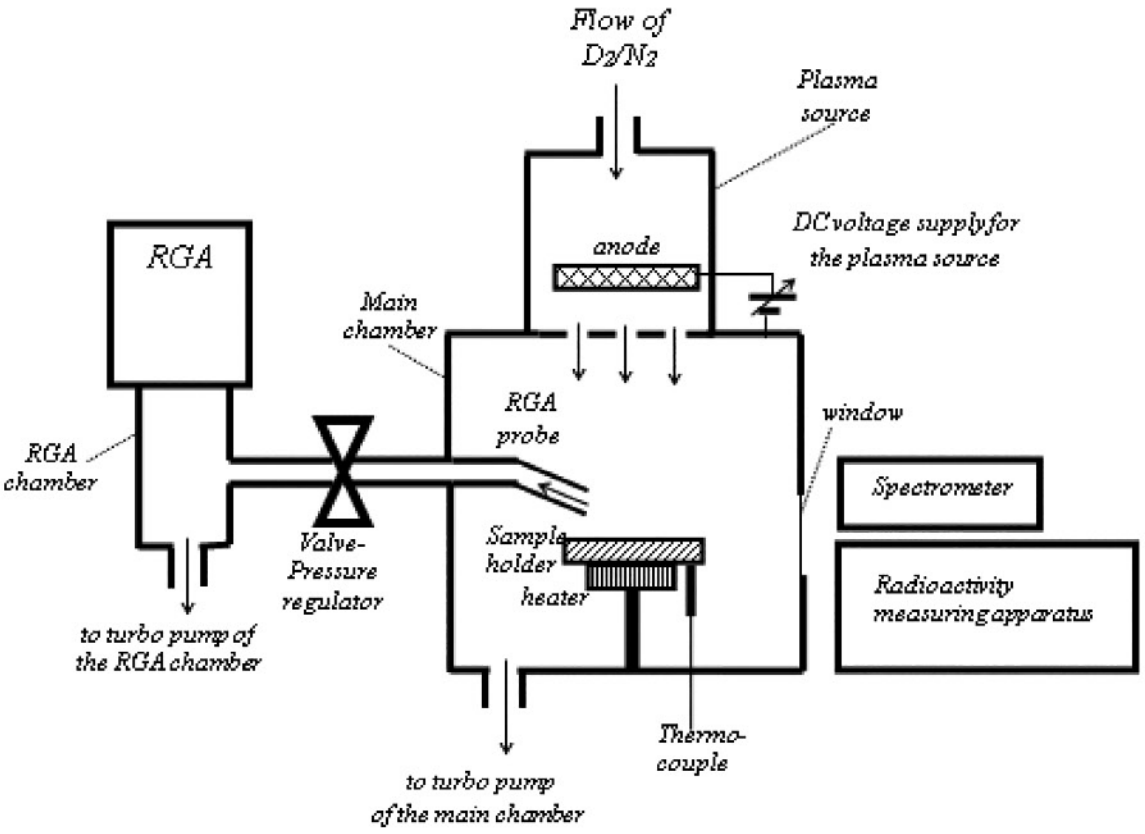

FIGURE 1 Experimental scheme

provides opportunity for the temperature of the sample holder to be maintained in range from room temperature up to 800°C. The holder is connected to the main chamber by a thin rod in order for the impact of the chamber on the holder temperature to be minimized. The temperatures below 600°C were measured by the thermocouple and those above 600°C—by the pyrometer.

3. The RGA probe in the main chamber has closest position to the specimen (~3 cm above the specimen) in order to measure the gasses nearby the surface of the specimen.
4. The voltage of the DC plasma source can be maintained in range from ~10 V up to 1500 V, providing opportunity that the kinetic energies of ions to be changed in relatively wide range. The operation of the plasma source was maintained in a way in which sparking to be avoided during the experiments involving low-temperature plasma.
5. There is a hydrogen environment in the main chamber caused by parasitic-injected hydrogen.
6. The RGA equipment for atomic and molecular mass analysis can identify the gases and their corresponding pressures from $1*10^{-10}$ up to $1*10^{-5}$ Torr. (Please note, that the pressure in the RGA chamber cannot be greater than $\sim 10^{-5}$ Torr in order for the used mass spectroscopy equipment to operate. The real pressures of the gasses in the main chamber section were greater, and there was pressure reduction between both chambers that are connected with a pipe and a pressure regulator.)
7. The equipment for optical spectroscopy can make measurements of spectral magnitudes in an optical wave range from 180 up to 880 nm.
8. The detector PRM1703GN for neutrons and for γ-rays has range from 1 up to 99 n/s for neutrons and range from 1 μR/hr up to 9999 μR/hr for γ-rays, and the detector RADIAC SET AN/UDR-13 for α-, β-, and γ-rays has range from 0.001 up to 1000 (in units 0.01 of Gray/hr).
9. The pressures in both main and RGA chambers are maintained by computer-controlled valves and by turbo-pumps, and no contaminations of oil products can be expected in both chambers.
10. The position of the DC plasma source is separated in terms of the main chamber, and the connection is through holes in the cathode of the plasma source. The injected gas stream (either plasma or non-plasma) flows from the plasma source to the main chamber, and, due to this reason, gasses created in the main chamber cannot reach the plasma source and cannot be part of the gasses where electrical discharge may take place.

Picture of a part of the system including the loading lock, the main chamber, and the plasma source is given in Figure 2.

The measuring apparatus were calibrated before the beginning of each experiment.

The mass-spectroscopy measurements (Figure 3) were done in the RGA histogram mode, which is the most accurate mode doing average of measured values, and these measurements were accepted in a way, in which they were shown. In case of injection of nitrogen gas only, these measurements show reasonable amounts of parasitic-injected gasses that are typical for the environment, that is, O, O_2, H_2O (Figure 4), and also they show that the amounts of both parasitic-injected ^3He and ^4He are less than 10^{-10} Torr in the RGA chamber that makes both amounts to be less than 10^{-4} Torr in the main chamber and no impact of the parasitic injected ^3He and ^4He can be expected, because the observed synthesized amounts of both ^3He and ^4He are in range 10^{-2} - 10^{-1} Torr.

The mass-spectroscopy measurements must be treated in the following way:

1. RGA score pertaining to one mass unit corresponds to atomic hydrogen (H);
2. RGA score pertaining to two mass units corresponds to both molecular hydrogen (H_2) and atomic deuterium (D);
3. RGA score pertaining to three mass units may correspond to: ^3He, H_3^+ ion, atomic T (tritium), and DH (deuterium hydride). However:

- If H_3^+ ion exists, then it is reasonable to expect existence of D_3^+ ion (six mass units), but there is no RGA

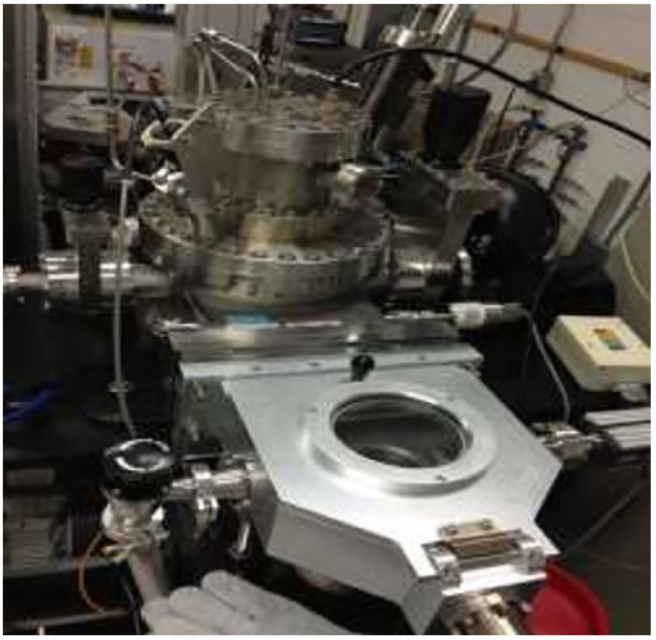

FIGURE 2 Picture of the part of the experimental equipment [Colour figure can be viewed at wileyonlinelibrary.com]

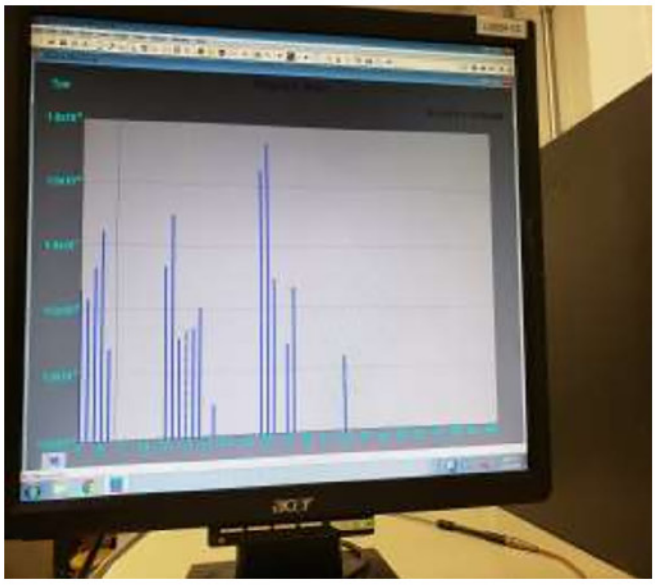

FIGURE 3 Residual gas analyzer in case of injection of N_2/D_2 gases [Colour figure can be viewed at wileyonlinelibrary.com]

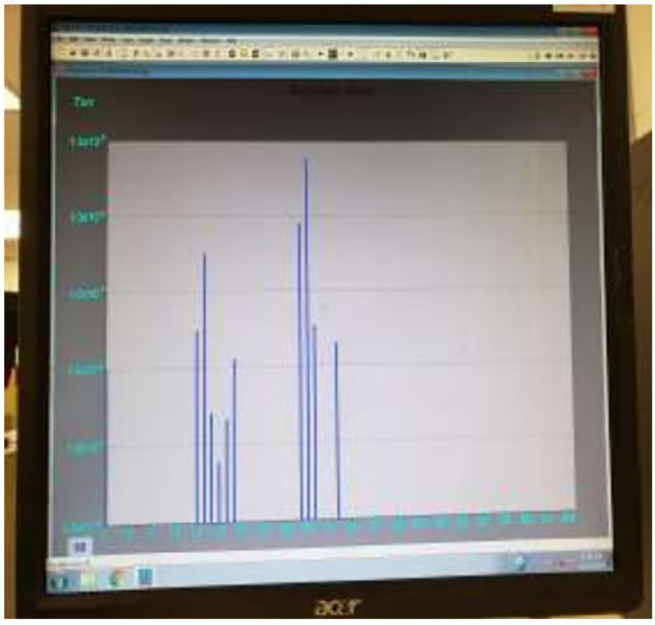

FIGURE 4 Residual gas analyzer in case of injection of N_2 gas [Colour figure can be viewed at wileyonlinelibrary.com]

score pertaining to six mass units, that is, this RGA score does not pertain to H_3^+ ion;

- If atomic T exists, then it is reasonable to expect that molecular T_2 to exist (six mass units), but there is no RGA score pertaining to six mass units, that is, this RGA score does not pertain to atomic T. (The lack of T also means that DT molecule—five mass units—does not have place.);
- If DH exists, then it is reasonable to expect that its amount must be less than or at least equal to the amounts of either H or H_2, but the RGA score pertaining to three mass units shows amount few times greater than the amounts of both H and H_2. From other side, if there is synthesis of DH, then it is reasonable that the increase of DH to cause decrease of H, or of H_2 or of both, which did not happen during the experiments, and the amount of H remained almost unchanged. Both (Figures 3 and 4) show that the contents of hydrogen (both atomic and molecular) and of water are much low than the shown RGA signal pertaining to the three mass units (Figure 3). Due to this reason, they cannot be considered to be some sources of hydrogen for a possible DH because the amount of the final product cannot be greater than the initial amounts of the constituents. Also, there was not organic matter on the surfaces, and the experiments were carried out after days in which the metal surfaces of the main chamber were exposed on vacuum in range $\sim 10^{-6}$ Torr, that is, complete degassing has been made before the experiments. Due to the above, it cannot be concluded that this RGA score corresponds to DH;

Conclusion: RGA score pertaining to three mass units corresponds to ^{3}He.

Reasonable questions (Q.) and corresponding answers (A.):

Q.: Is it possible that ^{3}He to be subject to a possible measuring error in RGA?

A.: No. Because if it is a case, the amounts of the neighboring scores corresponding to two mass units and to four mass units would be affected in similar ways due to changes in the experimental circumstances, but these amounts were not affected as it will be seen below

Q.: Is it possible that ^{3}He to be injected from outside of the main chamber?

A.: No. Because if it is a case, in the experiments, the amount of ^{3}He would change in the same way like the amounts of the injected D, D_2, and N_2, but it did not as it will be seen below. As it is shown above, both Figures 3 and 4 show that a parasite injected ^{3}He does not impact the synthesized ^{3}He.

Q.: Is it possible that ^{3}He to be product of a chemical reaction?

A.: No. Because if it is a case, initial chemical compounds containing ^{3}He must be subjected to mass-spectroscopy detections, and they were missing.

Conclusion: ^{3}He is a product of cold nuclear fusion reaction in the main chamber (ν_{an} is antineutrino).

$$D + D \rightarrow {}^3He + (\text{nuclear products}) + \nu_{an} + (\text{energy}) \quad (1)$$

It must be noted that normally (nuclear products) in (1) can be considered to be neutron. However, as it mentioned above, one developed new theory that shows different nuclear products. Because this theory will be published separately, one is not going to specify the exact content of (nuclear products) because any specification cannot be defended without the developed theory.)

4. RGA score pertaining to four mass units corresponds to both ^{4}He and D_2 (this RGA apparatus cannot distinguish both gasses.)
5. RGA score pertaining to five mass units may correspond to: $^4HeH^*$ (excited stable helium hydride molecule), DT molecule, and D_2H^+ stable positive ion. However:

- If DT molecule exists, then also molecular T_2 (six mass units) must exist, but there is no RGA score pertaining to six mass units, that is, this RGA score does not correspond to DT molecule;
- If D_2H^+ stable positive ion exists, then it is reasonable to expect that D_3^+ stable positive ion to exist, but as already it was mentioned, there is no RGA score pertaining to six mass units, that is, this RGA score does not correspond to D_2H^+ stable positive ion.

Conclusion: RGA score pertaining to five mass units corresponds to $^4HeH^*$.

Reasonable question and corresponding answer: Is the $^4HeH^*$ injected from outside? No, because as it will be seem below, $^4HeH^*$ does not show behavior of an injected gas with increase of the pressure of the main chamber such as nitrogen, that is, it is subject to chemical reaction in the main chamber. This behavior of $^4HeH^*$ also shows that ^{4}He is subject to creation in the main chamber, that is, it is not injected from outside (or at least the dominating part of ^{4}He has been synthesized in the main chamber), otherwise (ie, if ^{4}He was injected) it would form also $^4HeH^*$ outside the main chamber, and the $^4HeH^*$ amount would increase with increase of the amounts of the injected gasses, which did not happen in all experiments.

Conclusion: ^{4}He (or at least its dominating part) has been created in the main chamber as product of cold nuclear fusion reaction in the main chamber.

$$D + D \rightarrow {}^4He + \text{energy} \quad (2)$$

The developed new theory about cold nuclear fusion in solids explains the necessary conditions about existence of reaction (2) and the necessary conditions about the existence of the reaction (1). Both types of conditions cannot be described in this article because they cannot be defended in the absence of the developed theory, which will be published separately.

In the explanations above, one assumes that DH, D_2H^+, and H_3^+ can be synthesized in the main chamber, although the required conditions about synthesis of these molecules are different according to the literature.

3 | EXPERIMENTAL DATA ABOUT LOW-ENERGY NUCLEAR FUSION REACTION IN PALLADIUM NANOWIRES

Two specimens were used in the experiments: (a) Specimen 1 having 5.08 cm diameter—palladium nanowires technologically formed on aluminium substrate. This specimen was used for experiments at room temperature; and (b) Specimen 2 having 5.08 cm diameter—palladium nanowires technologically formed on stainless steel substrate. Specimen 2 was used for experiments at higher temperatures. The dissociation of a hydrogen molecule into hydrogen atoms on the Pd surface at room temperature is given in Reference 20, and it shows that hydrogen atoms can penetrate into the Pd specimen at both the room temperature and the higher one.

3.1 | Experiments with the Specimen 1

Graphs about synthesized ^{3}He and ^{4}He as function of the pressure in the main chamber at room temperature for Specimen 1 are provided in Figures 5–7. The following conclusions can be made according to the graphics:

1. The amounts of atomic H remain almost unchanged with increase of the pressure in the main chamber, which means the following: the atomic H is parasitic injected; the atomic H does not react with other gasses (including D), and it is reasonable to conclude that there is no chemical synthesis of DH. (In fact, the RGA score pertaining to three mass units changes, but the RGA score of H does not.);
2. The amounts of H_2/D change in a consistent way with the amounts of ^{4}He/D_2 and a reasonable conclusion that it is due to change of atomic D, that is, there is no reason to conclude that the H_2 amount changes. This outcome and the above outcome about H indicate that there is no reason to conclude about chemical synthesis of DH;

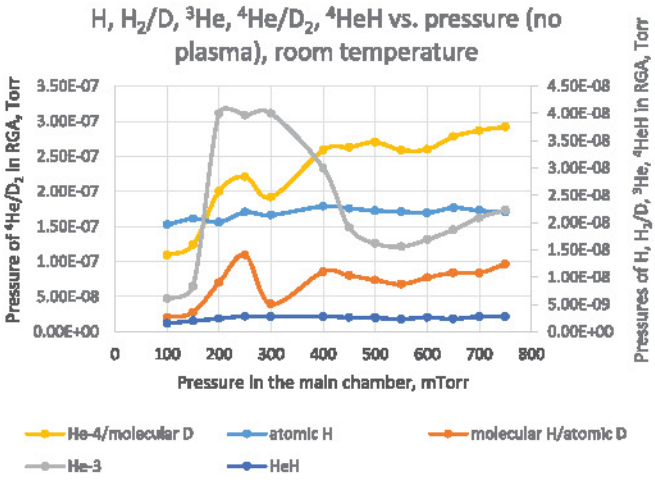

FIGURE 5 Mass spectroscopy for room temperature at nonplasma mode [Colour figure can be viewed at wileyonlinelibrary.com]

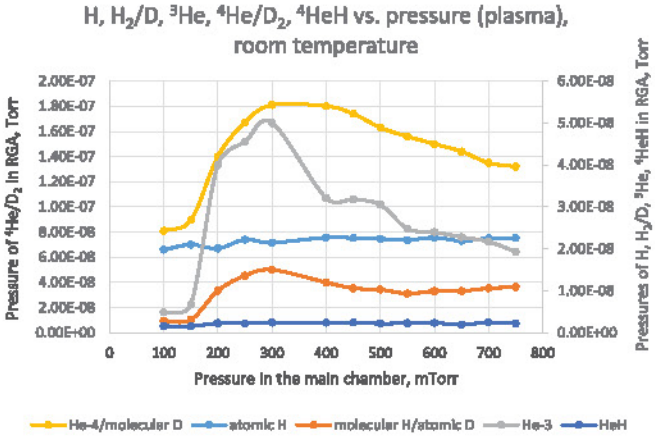

FIGURE 6 Mass spectroscopy at room temperature at plasma mode [Colour figure can be viewed at wileyonlinelibrary.com]

3. The amounts of ^{3}He change. Initially, these amounts increase reaching maximum values and after that they decrease. This behavior shows in addition that ^{3}He has been synthesized in the main chamber. In fact, the decrease is due to gas saturation of the specimen as new increase is possible only after degassing of the specimen. (One has developed a degassing technology that performs degassing for no longer than 3 minutes.) The degassing of the specimen is important in terms of replicability of the experiment. Before the gas saturation of the specimen, the amounts of ^{3}He are few times greater than the amounts of both H and H_2/D. Also the plasma mode provides increase of the ^{3}He amount in comparison with the nonplasma mode, and this increase is connected with decrease of $^4He/D_2$ amount, which means that D_2 is involved in the synthesis of ^{3}He according to (1). The increase of the ^{3}He amount in plasma mode means that the plasma stimulates ^{3}He synthesis, which can be explained by increase of penetration of deuterium particles in the specimen due to increase of their kinetic energies;
4. The amounts of $^4He/D_2$ in the nonplasma mode are greater than the corresponding amounts in the plasma mode, and it is connected with the increase of the ^{3}He amount in plasma mode, which means that the deuterium atoms participate in reaction (1). Also one assumes that there is decrease of the amount of ^{4}He that is subject to reaction (2) due to increase of deuterium amount engaged in reaction (1) as it will be confirmed below on a basis of $^4HeH^*$.
5. The amounts of $^4HeH^*$ in nonplasma mode are greater than those in plasma mode, and it is consistent with the conclusions in d about the amounts of ^{4}He. From the other side, the change of $^4HeH^*$ confirms the synthesis of ^{4}He according to reaction (2).

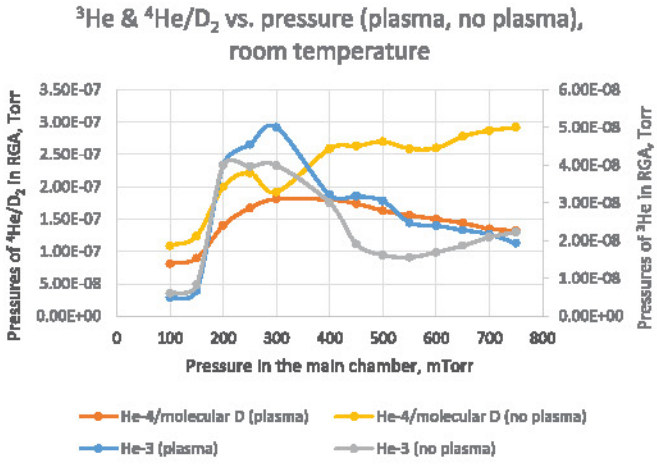

FIGURE 7 Mass spectroscopy about ^{3}He in both plasma and nonplasma modes [Colour figure can be viewed at wileyonlinelibrary.com]

3.2 | Experiments with the Specimen 2

Graphs regarding synthesized ^{3}He as a function of the pressure in the main chamber for four different temperatures of Specimen 2 are given in Figure 8 and in Figure 9. The experiments were made in sequence as the temperature increased. The following conclusions can be done:

1. At temperature 25°C, almost there is no difference in the ^{3}He amounts for both plasma and nonplasma modes. In both modes, the ^{3}He amounts decrease, which is connected with gas saturation of the specimen;

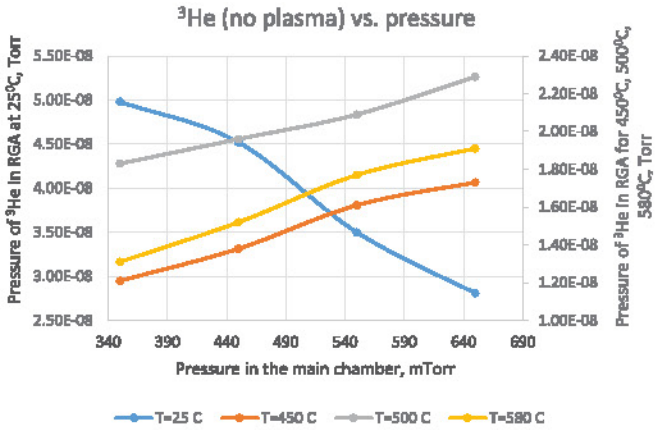

FIGURE 8 ^{3}He versus pressure in the main chamber for four temperatures at nonplasma mode [Colour figure can be viewed at wileyonlinelibrary.com]

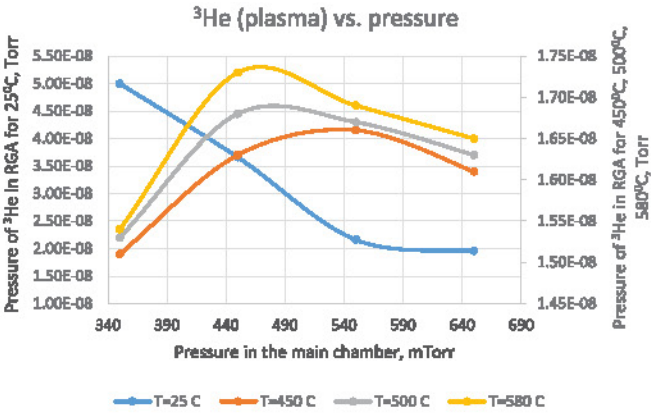

FIGURE 9 ^{3}He versus pressure in the main chamber for four temperatures at plasma mode [Colour figure can be viewed at wileyonlinelibrary.com]

2. At higher temperatures, the ^{3}He amounts in nonplasma mode increase with increase of the pressure, which is connected with partial degassing of the specimen with increase of the temperature. The same amounts in plasma mode reach certain maxima and after that decrease, which may be connected with deeper penetration of deuterium ions in the specimen due to increase of their kinetic energies, and, as a result, the degassing becomes more difficult.

Similar measurements show existence of synthesized ^{4}He, and the following conclusions can be made on the basis of these measurements:

1. Synthesis of ^{4}He is confirmed by presence of $^{4}HeH^{*}$, and the experimental outcomes here are the same as those for the Specimen 1 given above about both nonplasma and plasma modes;
2. Increase of the pressure gives increase of the ^{4}He amounts as it is connected with partial degassing of the specimen at higher temperatures.

However, it must be noted that presence of $^{4}HeH^{*}$ in the above experiments about both the specimen 1 and the specimen 2 has only qualitative meaning, and it proofs the synthesis of ^{4}He in the main chamber. The chemical synthesis of $^{4}HeH^{*}$ must be investigated further in order for a quantitative correlation between the amounts of both $^{4}HeH^{*}$ and ^{4}He to be determined and the released amount of ^{4}He to be found on this basis. Because in the circumstances of the above experiments, the released amounts of ^{4}He cannot be distinguished from $^{4}He/D_2$ and the impact of other factors such as temperature and plasma on the synthesis of ^{4}He cannot be determined. That is why one assumes that there was gas saturation of the specimens, and this saturation decreases the amount of the synthesized ^{4}He, however, it could not be determined by the experimental scheme in Figure 1.

4 | EXPERIMENTAL DATA ABOUT LOW-ENERGY NUCLEAR FUSION REACTION IN MOLYBDENUM (MO) METAL

Specimen of solid Mo metal having diameter 10.16 cm was placed on the sample holder. According to References 21,22, dissociation of hydrogen molecule into hydrogen atoms on the Mo metal surface has place at room temperature (and higher temperatures) as the hydrogen atoms penetrate by diffusion into the Mo specimen. Mass spectroscopy measurements were done, and the results are provided below.

4.1 | ^{3}He and its dependences

Dependences ^{3}He versus pressure in the main chamber are measured for plasma mode and for no plasma mode. The measuring scheme included: degassing of the specimen—pressure establishment—measurement at no plasma mode—measurement at plasma mode—new pressure establishment.... The time for performance of the measurements after the degassing was ~5 minutes for certain pressure, as no time for relaxation between different pressures was considered, that is, it is possible that residual impact of previous condition on ^{3}He generation of next condition can be expected. It was found in the experiments that the pressure increase in the main chamber gives increase of ^{3}He as it could be expected, despite fluctuations appear at higher pressures and residual effects may be reason about this. Also, it was found in

the experiments that at higher pressures, the ^{3}He amounts in plasma mode are normally greater than the ^{3}He amounts in no plasma mode, and it can be observed for plasma voltages less than 100 V.

Using the above scheme, experiments were done for plasma voltages greater than 100 V. Dependences of ^{3}He versus pressure (100-600 mTorr) in the main chamber are given in Figure 10 for plasma mode at 1000 V and for no plasma mode. Graph giving the plasma power versus pressure is provided as well. As it can be seen, the plasma power impacts the ^{3}He synthesis. Also, it can be seen within a pressure interval that ^{3}He synthesis at no plasma mode is greater than this at plasma mode, and one considers that residual effect has place. The increase of the plasma power at fixed voltage within a pressure interval in Figure 10 is connected with both increase of ion concentration and increase of ion velocity. One considers that the increase of the amount of generated ^{3}He within this interval is due to increase of the kinetic energy of the D ions penetrating into the Mo specimen. Similar characteristics were observed in other experiments having wider pressure interval (100-2000 mTorr). The graphs about ^{3}He in Figure 10 can be divided in two parts—one part (up to ~500 mTorr) where the plasma dominates in synthesis of ^{3}He and second part (greater than ~500 mTorr) where the increase of the pressure causes increase of the ^{3}He amount.

Both the minima and the maxima in Figure 10 do not have places in the experiments excluding the plasma mode. In this case, increase of the ^{3}He amount follows the increase of the pressure in the main chamber.

Experiments without degassing of the specimen were carried out as the outcomes have been used as basis for further experiments about heat release in the specimen. In case of no plasma mode, increase of the pressure in the main chamber causes increase of the ^{3}He amount. The experiments at plasma mode were carried out at pressures for which the increase of the plasma voltage causes increase of the plasma power and strong increase of the ^{3}He amount was observed with increase of the plasma power that is connected with increase of the kinetic energy of the D ions penetrating into the Mo specimen.

The graphs in Figure 11 pertain to experiment about ^{3}He synthesis as function of the temperature of the sample holder externally heated. The observed initial decrease of the ^{3}He amount is residual effect of initial degassing of the specimen (not all values pertaining to measurements immediately after degassing are provided, only the last four are given). After that increase of the ^{3}He amount with increase of the temperature can be observed.

The data provided in Figure 12 pertain to residual ^{3}He synthesis after stopping the primary established conditions (pressure, plasma voltage, and plasma power) in the main chamber. The measurements began without degassing of the specimen and continued until the shown ^{3}He amount became zero. No gas flow in the main chamber had place during the experiments, and the pressure in the main chamber was ~10^{-4} Torr, which created condition about extraction of incorporated deuterium and helium from the metal.

Based on the above, one has concluded that there were cold nuclear fusion reactions giving synthesis of ^{3}He in the Mo specimen, and the ^{3}He amount depends on the pressure in the main chamber, on the plasma power (for experiments at plasma mode) and on the temperature of the specimen.

4.2 | $D_2/^4$He gases and their dependences

Although the measuring equipment cannot distinguish D_2 from ^{4}He, one considers an importance of these measurements as generated ^{4}He can be part of $D_2/^4$He. The experiments were carried out at different temperatures of

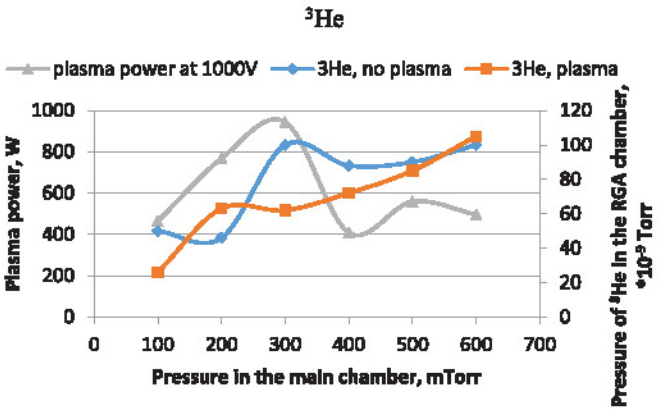

FIGURE 10 ^{3}He versus pressure in the main chamber and the plasma power [Colour figure can be viewed at wileyonlinelibrary.com]

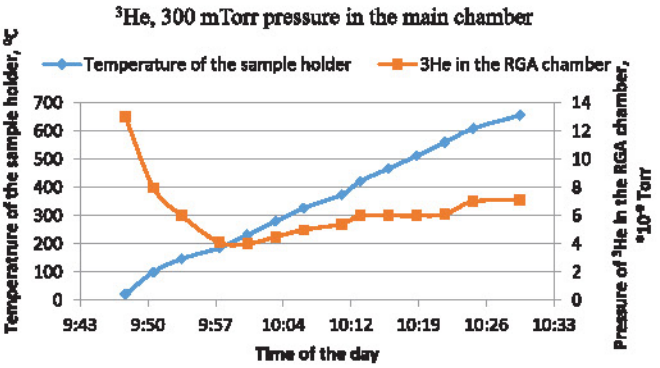

FIGURE 11 ^{3}He versus the temperature of the sample holder in the time [Colour figure can be viewed at wileyonlinelibrary.com]

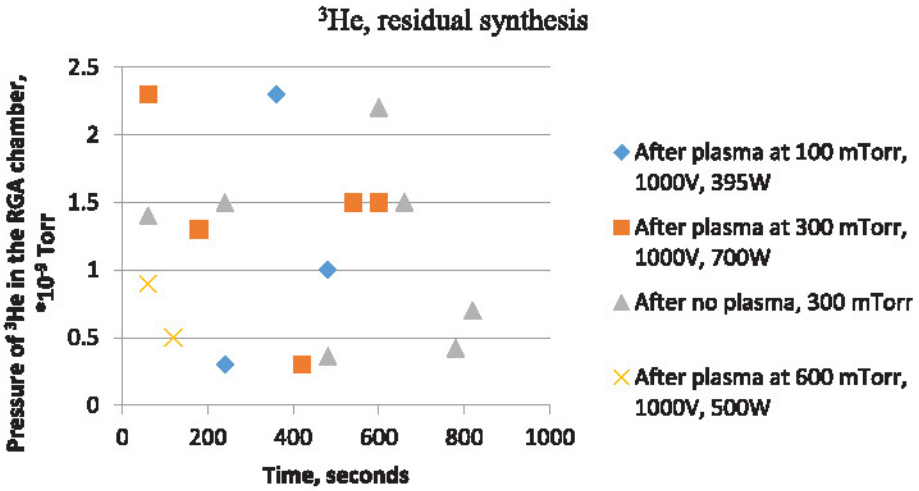

FIGURE 12 ^{3}He residual cold nuclear fusion synthesis versus the time [Colour figure can be viewed at wileyonlinelibrary.com]

the Mo specimen in two modes—without plasma and with plasma. The pressure of N_2/D_2 in the main chamber was regulated manually.

4.2.1 | Experiments without plasma

No plasma was considered for the experiments presented in this paragraph. The pressures of $D_2/^{4}$He as functions of the pressures in the main chamber for different externally established temperatures of the sample holder are measured. As it was reasonably expected, the pressure of $D_2/^{4}$He increases with increase of the pressure of N_2/D_2 in the main chamber. However, it was found that both graphical dependences are not parallel as the increase of the $D_2/^{4}$He is slower than the increase of the pressure in the main chamber. Also, the increase of the temperature of the specimen was done subsequently without degassing of the specimen before each temperature, and it was found experimentally that the total amount of $D_2/^{4}$He decreases in the time.

4.2.2 | Experiments with plasma

The experiments with plasma for externally established temperature of the sample holder were carried out at voltage 800 V as the plasma power varied in range 230 to 500 W depending on the pressure in the main chamber. All experiments show increase of the $D_2/^{4}$He amount with increase of the pressure in the main chamber. However, it is difficult that the impact of the plasma on the $D_2/^{4}$He amount to be estimated.

4.3 | $^{4}HeH^{*}$ gas in the system

Dependences of the $^{4}HeH^{*}$ gas on the times of the day and on the pressure in the main chamber (150-1100 mTorr) for four different temperatures (room temperature, 190°C, 377°C, and 657°C) of the sample holder were determined experimentally. The following conclusions can be made on basis of these measurements: (a) There are cyclic dependence of the amount of $^{4}HeH^{*}$ gas on the time including maxima and minima and (b) it cannot be made a conclusion that the pressure of $^{4}HeH^{*}$ gas depends on the pressure in the main chamber.

Based on the above, one has made conclusion that the pressure of the $^{4}HeH^{*}$ gas depends on the time, and the impact of other parameters is minor. Also one has made conclusion that the generation of $^{4}HeH^{*}$ gas is connected with the generation of ^{4}He in the system and the graphics in Figure 13 (for pressure in the main chamber 200 mTorr and room temperature) confirm it as the change of $^{4}HeH^{*}$ follows almost exactly the change of $D_2/^{4}$He.

4.4 | Temperature of the Mo specimen and both $D_2/^{4}$He and ^{3}He vs the time

Measurements of both the temperature of the Mo specimen and the change of concentration of $D_2/^{4}$He versus the time were performed. The same measurements were performed for ^{3}He. For the first experiment, the pressure in the main chamber was maintained to be 200 mTorr, and the same pressure for the second experiment was 1200 mTorr. No additional heating and no plasma were considered during the experiments. Both performed experiments had duration ~120 minutes. The graphical dependences of both $D_2/^{4}$He and the temperature are given in Figure 14 and the dependences of ^{3}He and temperature in Figure 15.

Comparison of the graphics in Figure 14 shows that there are changes vs the time, and that some correlation regarding the changes can be found as the cyclic behavior of both graphics can be determined. The ^{3}He graphic in Figure 15

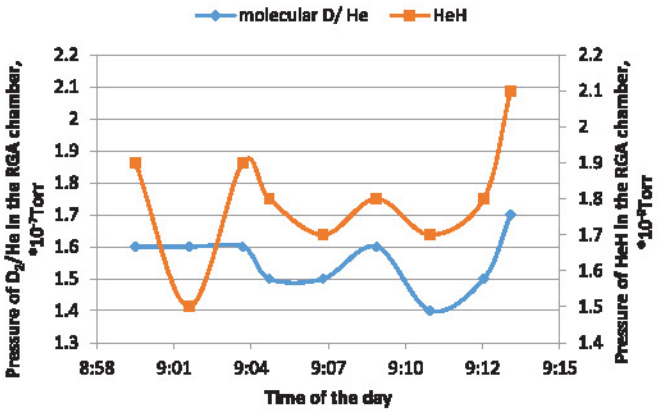

FIGURE 13 $^{4}HeH^{+}$ and $D_2/^{4}He$ versus time [Colour figure can be viewed at wileyonlinelibrary.com]

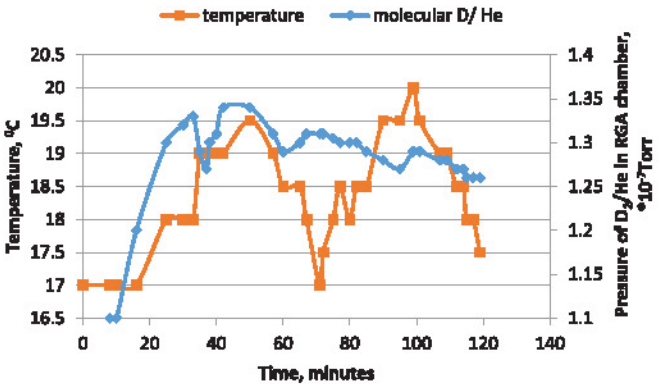

FIGURE 14 $D_2/^{4}He$ and temperature versus the time duration of the experiment [Colour figure can be viewed at wileyonlinelibrary.com]

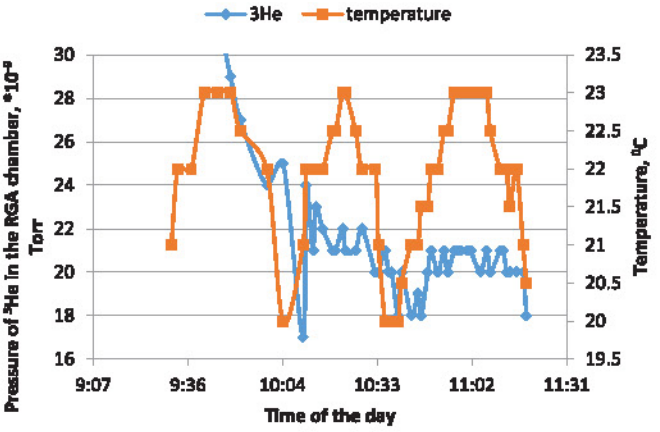

FIGURE 15 ^{3}He and the temperature versus the time of the day [Colour figure can be viewed at wileyonlinelibrary.com]

accommodates only part of the data in order for suitable scaling to be used, but in fact, the amount of the ^{3}He decreases after significant initial value following the degassing of the specimen as it was mentioned above. The graphics in Figure 15 show cyclic behavior correlation between both graphics. The released heat is determined on the basis that the temperature increases with 3°C during certain time interval, and the corresponding net energy released in the sample holder is 384.15229776 J for this time interval.

One can consider that synthesis of He (both ^{4}He and ^{3}He as it was shown above) in the specimen occurs, and it causes generation of heat. However, the maxima of $D_2/^{4}He$ and of ^{3}He decrease in the time and one explains this fact with incorporation of ^{4}He and of ^{3}He atoms in the Mo crystal lattice followed by local saturation and as result the synthesis of He decreases. Also, according to the experimental data, the temperature increases and one considers that it is connected with generation of He giving local release of significant energy that causes local destroying in the Mo crystal lattice. Recovery and reestablishment of the Mo crystal lattice is connected with decrease of He generation (and decrease of the local energy release). Reestablishment of the lattice leads to further increase of He generation and increase of released energy that causes further increase of the temperature. (It must be noted that the above recovery of the crystal lattice is partial and pertains only to the regions where the lattice has been destroyed due to cold nuclear fusion reaction. This recovery can happen at room temperature as no significant energy is required for the annealing process.)

The incorporation of deuterons in the Mo specimen is governed by the Fick's law of diffusion as clear diffusion from unlimited source took place. Due to this reason, it is not possible that a cyclic change of the temperature to take place if a reason for the heat release is absorption of deuterium in the Mo specimen as in this way the absorption of deuterium must be cyclic, which is in disagreement with the Fick's law of diffusion. And something else was observed in the cold nuclear fusion experiments that the heat release is in time phase with the amount of released ^{3}He, that is, if the ^{3}He amount increases, the temperature increases and vice versa. Due to this reason and according to the above about cold nuclear fusion synthesis of ^{3}He, it is considered that cold nuclear fusion origin of the heat release is the only reasonable explanation. Also, this explanation corresponds to the partial annealing recovery of the crystal lattice that was mentioned above.

5 | PLASMA OPTICAL SPECTRA

Optical spectra measurements of both plasma of nitrogen-deuterium mixture including nuclear-synthesized He gas and plasma of pure He gas only were performed for

pressures in range 100 to 1200 mTorr in the main chamber for different anode-cathode voltages varying in range 50 to 1000 V. These optical measurements were carried out for all types of specimens described above. The experimental results are the same for all experiments in terms of spectral positions of the spectral peaks as only the difference consists in the magnitudes of these peaks and that is why only one representative optical measurement for the Mo specimen is presented in the article.

The results for pressure 275 mTorr and voltage 800 V for plasma of nitrogen-deuterium mixture (including cold nuclear fusion synthesized He) are provided in Figure 16. The peaks—at 357.02, 390.18, 427.71, 501.23, and 667.81 nm—corresponding to He in the plasma of the nitrogen-deuterium gas mixture (including synthesized He) are given, and they are compared by alignment with peaks of pure He plasma at 1000 V. It can be seen in Figure 16 that some of the spectral peaks typical for the pure He plasma are no presented in the plasma of deuterium-nitrogen gas mixture containing synthesized He. This fact is an important additional proof (additional to the reported above mass spectroscopy measurements) about cold nuclear fusion synthesis of He, due to the following reasons: (a) As it can be seen from the experimental scheme of Figure 1, the plasma source is external in terms of the main chamber, and both apparatus are connected via a hollow cathode; (b) The electrical plasma discharge takes place only in the plasma source and affects only the gasses having place in the chamber of the plasma source because the gas stream has direction from the plasma source into the main chamber, and there is no way that gasses generated in the main chamber to reach the plasma source and to be affected by the electrical plasma discharge; (c) Due to (a) and (b) the excited particles from the plasma source, which are injected into the main chamber, cause secondary excitation of the gasses in the main chamber, and these new excited gasses have corresponding contributions to the optical plasma spectrum that can be measured through the window of the main chamber according to the Figure 1. In fact, in the circumstances of the above reported experiments, the excited particles of the deuterium-nitrogen plasma from the plasma source were injected into the main chamber and caused a secondary excitation for the He gas, which has been synthesized by cold nuclear fusion reaction in the main chamber. The secondary excited He gas made contributions to the optical spectrum only in certain optical spectral lines corresponding to the secondary excitations. Thus, the lack of some optical spectral lines of the pure He in the optical

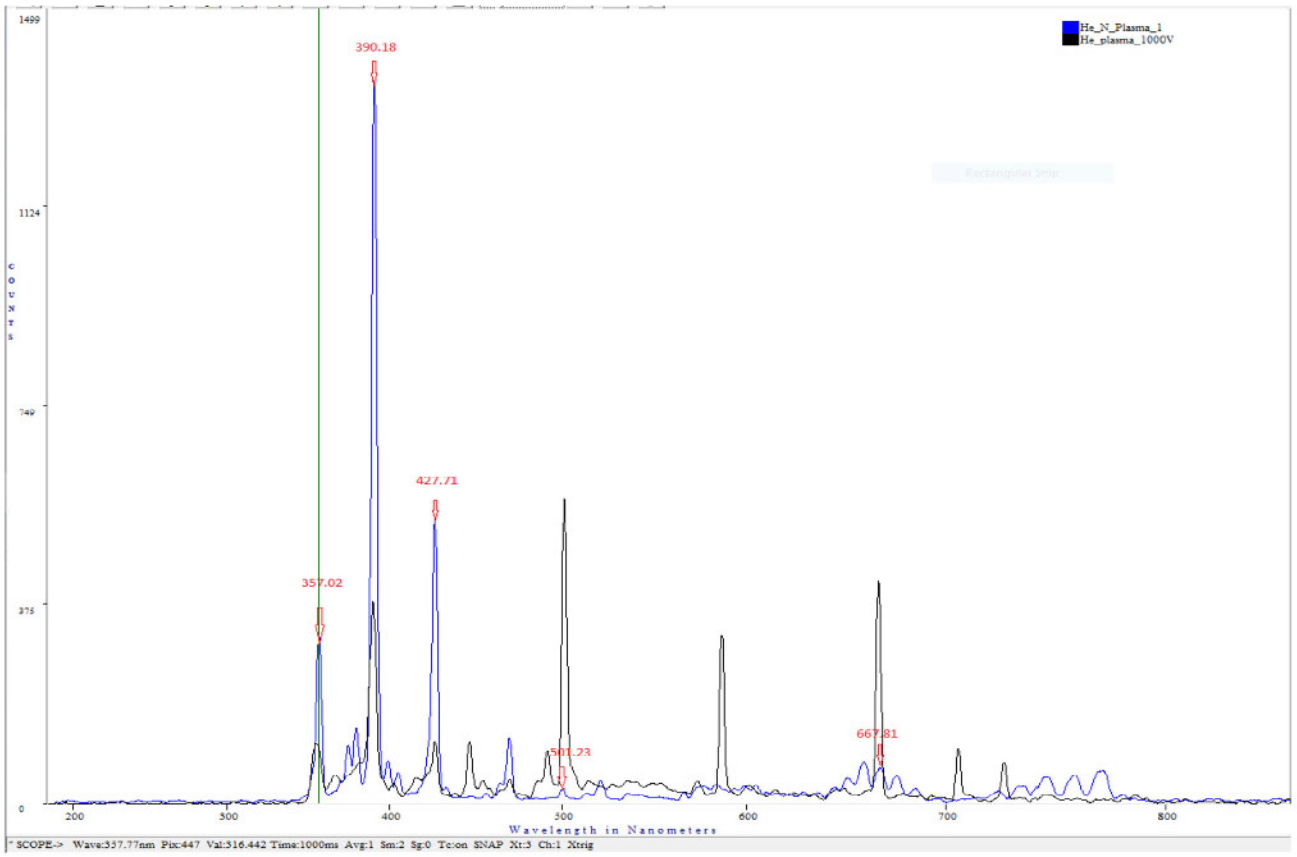

FIGURE 16 Peaks overlap in both He plasma only and D/N (including generated He) plasma [Colour figure can be viewed at wileyonlinelibrary.com]

spectrum of the deuterium-nitrogen plasma containing synthesized He can be considered as a proof that this He has been synthesized in the main chamber and that He has not been injected. There is only one way He to be synthesized in the main chamber—He is a product of cold nuclear fusion reaction of deuterium in its interaction with the metal specimen.

6 | MEASUREMENT OF RADIOACTIVITY DURING THE EXPERIMENTS

According to the experimental scheme of Figure 1, measurement of radioactivity was made during all experiments, and no radioactivity above the normal background was measured. No neutron radiation above the normal background was observed as it could be due to: (a) Low amounts of gases used in the experiments and relatively high thresholds of the used equipment for radiation measurements and/or (b) the energy of the released neutron has been low and the neutrons have not left the main chamber or even they have not left the specimens at all and/or (c) there is no neutron emission in the experiments carried out. However, one considers that the matter about the radiation has to be investigated in addition with more precise measuring equipment.

7 | HEAT RELEASE DURING THE EXPERIMENTS

Measurements of the temperature of the sample holder were made during the experiments carried out without additional heating. It was a relatively significant change of the temperature for the Mo specimen, and it was shown above. Also, cyclic change (in nonplasma mode) in the time was found as it was reported above. Changes in the temperatures of the sample holder were observed in experiments with the other specimens; however, they were not very well expressed as those for the Mo specimen, mainly due to their relatively low volumes.

8 | INVESTIGATION OF OTHER MATERIALS FOR LOW-ENERGY NUCLEAR FUSION REACTIONS

Also, one investigated specimens of other materials in terms of release of both synthesized ^{3}He and synthesized ^{4}He. The investigated specimens were metals gallium (Ga) and aluminum (Al). No release of both ^{3}He and ^{4}He was detected according to the above defined criteria for both mass-spectroscopy and optical spectroscopy.

9 | CONCLUSIONS

Experimental evidences about low-energy nuclear fusion reactions in Pd nanowires and in Mo solid metal are provided in this article. The evidences consider release of both synthesized ^{4}He and synthesized ^{3}He in interaction of deuterium gas with the above materials. The provided evidence about release of helium gas in these interactions are two types—mass spectroscopy and optical spectroscopy data. In addition, heat release in Mo specimen is reported as outcome of low-energy nuclear fusion reaction. It is determined that the released amount of the synthesized ^{3}He increases with increase of both the temperature of the specimen and the kinetic energy of the deuterium particles. No radiation in terms of both neutron emission and gamma ray emission was measured in the experiments.

DATA AVAILABILITY STATEMENT

The data that support the findings of this study are available on request from the corresponding author. The data are not publicly available due to privacy or ethical restrictions.

ORCID

Dimiter Alexandrov https://orcid.org/0000-0002-1319-4786

REFERENCES

1. Fleischmann M, Pons S. Electrochemically induced nuclear fusion of Deuterium. *J Electroanal Chem Interfacial Electrochem*. 1989;261:301-308.
2. Jones SE, Palmer EP, Czirr JB, et al. Observation of cold nuclear fusion in condensed matter. *Nature*. 1989;338:737-740.
3. Arata Y, Zhang YC. Solid-state plasma fusion ("cold fusion"). *J High Temp Soc*. 1997;23:1-56.
4. Gimzewski JK, Naranjo B, Putterman S. Observation of nuclear fusion driven by a pyroelectric crystal. *Nature*. 2005;434(7037):1115-1117.
5. Avino P, Santoro E, Sarto F, Violante V, Rosada A. Neutron activation analysis for investigating purity grade of copper, nickel and palladium thin films used in cold fusion experiments. *J Radioanal Nucl Chem*. 2011;290(2):427-436.
6. Arata Y. The basics of nuclear fusion reactor using solid Pycnodeuterium as nuclear fuel. *Prog Theor Phys Suppl*. 2004;154:241-250.
7. Kasagi J. Low energy nuclear cross sections in metals. *Surf Coat Technol*. 2007;201(19–20):8574-8578.
8. Novakovic L. Three-particle clusters and the cold-fusion problem. *Int J Hydrog Energy*. 2004;29(13):1397-1407.
9. Coraddu M, Lissia M, Mezzorani G, Quarati P. Fusion reactions in plasmas as probe of the high-momentum tail of particle distributions. *Eur Phys J B*. 2006;50(1–2):11-15.

10. Kimura S, Bonasera A, Cavallaro S. Effect of the electronic chaotic motion on the fusion dynamics between hydrogen isotopes. *Radiat Effects Defects Solids*. 2005;160(10–12):677-684.
11. Afonichev D. Mechanism of cold fusion via tritium channel. *Int J Hydrog Energy*. 2006;31(4):551-553.
12. Woo TH, Noh SW. Lattice squeezed nuclear reaction (LSNR) of power-cell for nanoscopic investigations using ion beam injections. *Int J Green Energy*. 2011;8(5):511-517.
13. Sinha K, Meulenberg A. Laser stimulation of low-energy nuclear reactions in deuterated palladium. *Curr Sci*. 2006;91(7):907-912.
14. Dufour J, Murat D, Dufour X, Foos J. Exothermic reaction induced by high-density current in metals: possible nuclear origin. *Int J Nucl Energy Sci Technol*. 2005;1(4):280-290.
15. Woo T, Cho H. Vacuum assisted ion injection using deuterium gas for nano-power cell production. *Int J Nucl Energy Sci Technol*. 2010;5(3):275-282.
16. Hora H, Miley G. Maruhn-greiner maximum of uranium fission for confirmation of low energy nuclear reactions LENR via a compound nucleus with double magic numbers. *J Fusion Energ*. 2007;26(4):349-355.
17. Kalman P, Keszthelyi T. Solid state modified nuclear processes. *J Appl Phys*. 2008;44(3):297-302.
18. Kalman P, Keszthelyi T. Solid state internal conversion, physical review C. *Nucl Phys*. 2004;69(3):031606(R).
19. Widom A, Larsen L. Ultra low momentum neutron catalyzed nuclear reactions on metallic hydride surfaces. *Eur Phys J C*. 2006;46(1):1007-1111.
20. D. A. Otterson, R. J. Smith. *Absorption of Hydrogen by Palladium and Electrical Resistivity Up To Hydrogen-Palladium Atom Ratios 0.97*, NASA Technical Note D-5441, Washington, DC, USA, September 1969
21. Tanabe T, Yamanishi Y, Imoto S. Hydrogen permeation and diffusion in molybdenum. *J Nucl Mater*. 1992;191-194:439-443.
22. Frauenfelder R. Permeation of hydrogen trough tungsten and molybdenum. *J Chem Phys*. 1968;48(9):3955-3965.

How to cite this article: Alexandrov D. Low-energy nuclear fusion reactions in solids: Experiments. *Int J Energy Res*. 2020;1–13. https://doi.org/10.1002/er.6356